

Increased Cholesterol Content in Gammadelta ($\gamma\delta$) T Lymphocytes Differentially Regulates Their Activation

Hsin-Yuan Cheng¹, Runpei Wu¹, Abraham K. Gebre², Richard N. Hanna¹, Dan J. Smith³, John S. Parks², Klaus Ley¹, Catherine C. Hedrick^{1*}

1 Division of Inflammation Biology, La Jolla Institute for Allergy & Immunology, La Jolla, California, United States of America, **2** Department of Pathology/Lipid Sciences, Wake Forest School of Medicine, Winston-Salem, North Carolina, United States of America, **3** Targeson, Inc., San Diego, California, United States of America

Abstract

Gammadelta ($\gamma\delta$) T lymphocytes respond quickly upon antigen encounter to produce a cytokine response. In this study, we sought to understand how functions of $\gamma\delta$ T cells are differentially regulated compared to $\alpha\beta$ T cells. We found that cholesterol, an integral component of the plasma membrane and a regulator of TCR signaling, is increased in $\gamma\delta$ T cells compared to $\alpha\beta$ T cells, and modulates their function. Higher levels of activation markers, and increased lipid raft content in $\gamma\delta$ cells suggest that $\gamma\delta$ T cells are more activated. Cholesterol depletion effectively decreased lipid raft formation and activation of $\gamma\delta$ T cells, indicating that increased cholesterol content contributes to the hyper-activated phenotype of $\gamma\delta$ T cells, possibly through enhanced clustering of TCR signals in lipid rafts. TCR stimulation assays and western blotting revealed that instead of a lower TCR threshold, enhanced TCR signaling through ERK1/2 activation is likely the cause for high cholesterol-induced rapid activation and proliferation in $\gamma\delta$ T cells. Our data indicate that cholesterol metabolism is differentially regulated in $\gamma\delta$ T cells. The high intracellular cholesterol content leads to enhanced TCR signaling and increases activation and proliferation of $\gamma\delta$ T cells.

Citation: Cheng H-Y, Wu R, Gebre AK, Hanna RN, Smith DJ, et al. (2013) Increased Cholesterol Content in Gammadelta ($\gamma\delta$) T Lymphocytes Differentially Regulates Their Activation. PLoS ONE 8(5): e63746. doi:10.1371/journal.pone.0063746

Editor: Michael B. Fessler, National Institute of Environmental Health Sciences, United States of America

Received: January 28, 2013; **Accepted:** April 4, 2013; **Published:** May 21, 2013

Copyright: © 2013 Cheng et al. This is an open-access article distributed under the terms of the Creative Commons Attribution License, which permits unrestricted use, distribution, and reproduction in any medium, provided the original author and source are credited.

Funding: The work was supported by National Institutes of Health Grants P01HL055798 and R01HL097368 (to C.C.H.), R01HL049373 and R01HL094525 (to J.S.P.), and American Diabetes Association Mentor-Based Postdoctoral Fellowship 7-12-MN-31 (to H.-Y.C. and C.C.H.). The funders had no role in study design, data collection and analysis, decision to publish, or preparation of the manuscript.

Competing Interests: One of the co-authors of the manuscript, Mr. Dan Smith, is employed by Targeson, Inc., a commercial company. Another co-author, Dr. Klaus Ley, is a consultant, but is not employed by Targeson, Inc. However, their affiliation to the company does not alter the authors' adherence to all the PLOS ONE policies on sharing data and materials.

* E-mail: hedrick@liai.org

Introduction

Most T cells express the $\alpha\beta$ T cell receptor (TCR). However, a small subset of T cells expresses the γ and δ chains of the TCR. These $\gamma\delta$ T cells represent ~3–5% of total CD3⁺ T cells in human peripheral blood and recognize non-peptide antigens such as lipids and phosphorylated nucleotides, as well as antigens that do not require processing and presentation by MHC molecules [1,2]. Antigen-naïve $\gamma\delta$ T cells can react quickly, within hours after pathogen infection, and thus serve an innate immunity-like role before $\alpha\beta$ T cells and other adaptive immune responses could take place [2,3]. A $\gamma\delta$ T cell response is key to numerous pathogenic processes, as these cells have been shown to facilitate adaptive immune responses through various mechanisms [4]. For instance, $\gamma\delta$ T cells promote the maturation of naïve dendritic cells during viral infection, possibly through the production of proinflammatory cytokines such as TNF α , IFN γ , and IL-6 [5]. $\gamma\delta$ T cells are also shown to induce robust CD8⁺ T cell responses by cross-presenting microbial and tumor antigens to CD8⁺ T cells [6].

Several groups have investigated unique gene expression patterns of $\gamma\delta$ T cells upon stimulation as hallmarks to distinguish them from $\alpha\beta$ T cells, but have reported finding relatively similar expression profiles thus far [7,8,9]. One of the most noteworthy findings was by Fahrner et al., who reported that $\gamma\delta$ and $\alpha\beta$ T cells show distinct expression patterns of both lipid metabolism and

inflammatory genes upon *Y. pseudotuberculosis* infection [10]. These investigators reported that mRNA for several lipid metabolism genes were expressed only in the $\gamma\delta$ T cell samples. Another recent study reported that the response of $\gamma\delta$ T cells toward influenza virus was potently inhibited by blocking HMG-CoA reductase, the rate-limiting enzyme in cholesterol biosynthesis, suggesting sterol metabolism may be important for the function of $\gamma\delta$ T cells [11].

Cholesterol maintains proper permeability and fluidity of the mammalian cell membrane to ensure cell growth and function. Cholesterol plays a role in mediating signal transduction by assisting the formation of lipid rafts, the specialized microdomains for organizing signaling molecules [12]. However, cholesterol levels must be properly regulated as excess sterol results in adverse effects on normal cell functions as well as the development of diseases such as atherosclerosis. Several studies have demonstrated that the homeostasis and functions of various T cell subsets are strongly linked to cellular and environmental cholesterol levels. Resting peripheral CD4⁺ T cells and the Th1 responses were both increased after *in vivo* cholesterol enrichment [13]. Coincidentally, we also reported that CD4⁺ T cells had increased intracellular cholesterol content and proliferative advantage in the absence of ABCG1, an cholesterol efflux transporter [14]. On the other hand, proliferation of NKT cells in response to α GalCer stimulation was lower in hypercholesterolemic ApoE^{-/-} mice [15]. In this report, we provide novel evidence by which $\alpha\beta$ and $\gamma\delta$ T cells are

differentially regulated by intracellular cholesterol content. We found that intracellular cholesterol levels are basally elevated in $\gamma\delta$ T cells and that this contributes to their “primed for action” phenotype by favoring TCR clustering and signaling.

Methods

Mice

C57BL/6J (000664) mice were purchased from The Jackson Laboratory. Mice were fed a standard rodent chow diet and housed in microisolator cages in a pathogen-free facility. All experiments followed guidelines of the La Jolla Institute for Allergy and Immunology Animal Care and Use Committee, and approval for use of rodents was obtained from the La Jolla Institute for Allergy and Immunology according to criteria outlined in the Guide for the Care and Use of Laboratory Animals from the National Institutes of Health. Mice were euthanized by CO₂ inhalation.

Flow Cytometry

Spleens or peripheral lymph nodes (cervical, axillary, brachial, and inguinal) were excised and pushed through a 70- μ m strainer. Red blood cells were lysed in RBC Lysis Buffer according to the manufacturer’s protocol (BioLegend). All samples were collected in Dulbecco’s PBS (Gibco) with 2 mM EDTA and were stored on ice during staining and analysis. $2\text{--}6\times 10^6$ cells were resuspended in 100 μ l flow staining buffer [1% FBS plus 0.1% NaN₃ in PBS]. Fc receptors were blocked for 10 min and surface antigens were stained for 30 min at 4°C and washed twice with flow staining buffer. LIVE/DEAD Yellow Fixable Dead Cell Stain (Invitrogen) was used for analysis of viability, and forward- and side-scatter parameters were used for exclusion of doublets from analysis.

For measurement of intracellular lipids, after surface markers staining, cells were stained for an additional 15 min at room temperature with 5 ng/ μ l Nile Red (Enzo) and then washed twice.

For measurement of lipid rafts, cells were stained with Alexa Fluor 488-conjugated Cholera toxin subunit B (1/1000 dilution; Molecular Probes) together with other surface staining antibodies for 30 min at 4°C, and then washed twice.

Cellular fluorescence was assessed using LSR II flow cytometer (BD Biosciences) and percentages of subsets and median fluorescence intensity (MFI) were analyzed with FlowJo software (TreeStar version 9.2).

Fluorescence-labeled antibodies used were- anti-CD3 (145-2C11, eBioscience), anti-TCR β (H57-597, eBioscience), anti- $\gamma\delta$ TCR (eBioGL3, eBioscience), anti-CD69 (H1.2F3, BD Pharmingen), anti-CD44 (IM7, eBioscience), and anti-CD62L (MEL-14, eBioscience).

In vivo proliferation assay

C57BL/6J mice were intraperitoneally injected with 1 mg BrdU (BD Pharmingen). Spleens were harvested after 3 days, and BrdU incorporation was detected following manufacturer’s instruction (FITC BrdU Flow Kit, BD Pharmingen).

Quantification of cholesterol content

Splenocytes were isolated from C57BL/6J mice and stained with anti-CD3, -TCR β , - $\gamma\delta$, and LIVE/DEAD Yellow Fixable Dead Cell Stain (Invitrogen). 3 spleens were pooled per sample. Stained cells were sorted into $\alpha\beta$ (live, CD3⁺, TCR β ⁺, and $\gamma\delta$ ⁻) and $\gamma\delta$ (live, CD3⁺, $\gamma\delta$ ⁺, and TCR β ⁻) T cells by FACSaria flow cytometer (BD Biosciences). $\sim 9\times 10^6$ $\alpha\beta$ T cells and $\sim 1.5\text{--}2\times 10^5$ $\gamma\delta$ T cells were collected per mouse sample. 6×10^5 $\alpha\beta$ and all of the $\gamma\delta$ T cells ($\sim 1.5\text{--}2\times 10^5$) were used for GC quantification.

After several washes with PBS, the cell pellet was extracted with isopropanol containing 5-cholestane as internal standard. Total and free cholesterol content was determined by gas-liquid chromatography and normalized to cell numbers, as previously described [16]. Cholesteryl ester was calculated as (total cholesterol - free cholesterol) $\times 1.67$. Multiplying by 1.67 corrects for the average fatty acid mass that is lost during saponification.

Quantification of cell size

$\alpha\beta$ and $\gamma\delta$ T cells were isolated by cell sorting as described in the quantification of cholesterol content. Diameters of single cells were measured by Multisizer IV Coulter Counter (Beckman Coulter).

PCR array

Splenocytes were isolated from C57BL/6J mice. Untouched T cells were purified by Pan T Cell Isolation Kit II (Miltenyi Biotec), and were then separated into $\alpha\beta$ and $\gamma\delta$ T cells by TCR γ/δ ⁺ T Cell Isolation Kit (Miltenyi Biotec). Spleens from 6 mice were pooled per sample. The purity of cells was assessed by flow cytometry and was above 90%. Total RNA was collected with the RNeasy Plus Micro Kit according to the manufacturer’s protocol (Qiagen). RNA purity and quantity was measured with a nanodrop spectrophotometer (Thermo Scientific). 150 ng RNA was used to for cDNA synthesis with RT² First Strand cDNA Kit (SABiosciences). Gene expression was detected using Lipoprotein Signaling & Cholesterol Metabolism PCR Array (PAMM-080, SABiosciences). Relative gene expression was analyzed using $\Delta\Delta C_t$ based fold-change calculations. Expression level of $\alpha\beta$ T cells was set as 1.

Quantitative RT-PCR

Magnetic beads purified $\alpha\beta$ and $\gamma\delta$ T cells from C57BL/6J splenocytes and total RNA extraction were stated above. Spleens from 3–4 mice were pooled per sample. 100 ng RNA was used for cDNA synthesis with iScript cDNA Synthesis Kit (Bio-Rad). mRNA expression was measured in real-time quantitative PCR using the following predesigned TaqMan gene expression assays (Applied Biosystems): *Abca1* (Mm01350760_m1), *Pcsk9* (Mm01263610_m1), *Acat1* (Mm00486279_m1), *Acat2* (Mm00448823_m1), *Lcat* (Mm00500505_m1), *Treml1* (Mm00553936_m1). Samples were assayed on a LightCycler 480 Real-Time PCR System (Roche). Threshold cycles (C_T) were determined by an in-program algorithm assigning a fluorescence baseline based on readings prior to exponential amplification. Fold change in expression was calculated using the $\Delta\Delta C_t$ method with *Gapdh* as an endogenous control. Expression level of $\alpha\beta$ T cells was set as 1.

Confocal microscopy imaging

$\alpha\beta$ and $\gamma\delta$ T cells were isolated from female C57BL/6J mice using magnetic beads as stated in the PCR array section above. Cells were stained with Alexa Fluor 488-conjugated Cholera toxin subunit B (1/1000 dilution; Molecular Probes), washed twice with PBS, and spun unto glass slides. Slides were imaged with a FluoView FV10i confocal laser-scanning microscope (Olympus).

In vitro cholesterol loading and depletion

C57BL/6J splenocytes were stimulated with Dynabeads mouse T-activator CD3/CD28 beads (Invitrogen) at 1 bead: 1 cell ratio in the absence or presence of 1 mM methyl β -cyclodextrin (Sigma-Aldrich) to deplete cholesterol, or 10 or 20 μ g/ml cholesterol-loaded cyclodextrin (Sigma-Aldrich) to load cells with cholesterol

for 2 or 4 hours. Cells were then removed from beads, stained for lipid rafts and activation markers, and analyzed by flow cytometry as described above.

In vitro T cell stimulation and proliferation assay

Splenocytes isolated from C57BL/6J mice were stained with 2.5 μ M CFSE (Invitrogen) for 10 min at 37°C, and washed extensively. Cells were then plated at 5×10^5 cells/well in a 96-well U-bottomed plate pre-coated with various concentrations of α CD3 antibody (BD Pharmingen). Soluble α CD28 antibody (BD Pharmingen) was added at 1 μ g/ml. 24 hours later, cells were stained with surface markers, and CFSE dilution in $\alpha\beta$ and $\gamma\delta$ subsets was determined by flow cytometry. In some experiments, U0126 (Sigma-Aldrich) was added to cultures at 10 and 25 μ M to inhibit ERK1/2 phosphorylation.

Western Blotting

C57BL/6J splenocytes were sorted into $\alpha\beta$ (live, CD3⁺, TCR β ⁺, and $\gamma\delta$ ⁻) and $\gamma\delta$ (live, CD3⁺, $\gamma\delta$ ⁺, and TCR β ⁻) T cells. Spleens of 25 mice were pooled for sorting. All of the sorted $\gamma\delta$ T cells (4.3×10^6) and same number of $\alpha\beta$ T cells were divided into 2 equal portions for generation of both unactivated and activated samples. Cells were either left untreated or incubated with 20 μ g/ml α CD3 and α CD28 antibodies for 5 min at 37°C, and then cross-linked by 20 μ g/ml goat anti-hamster IgG (Invitrogen) for another 2 min at 37°C. Cells were then lysed with RIPA buffer (50 mM Tris, pH 7.4, 150 mM NaCl, 1 mM EDTA, 1 mM EGTA, 1 mM NaVO₄, 1 mM NaF, 0.5% NP40, 0.1% Brij35, 0.1% deoxycholic acid) and ultrasonication. Protein quantification was performed using BCA Protein Assay Reagent (Thermo Scientific). 30 μ g protein per sample was loaded into SDS-PAGE, and sequentially immunoblotted with the following antibodies: anti-phospho-ERK1/2 (1:250; Cell Signaling #4370), anti-ERK1/2 (1:1000; Cell Signaling #4695), and anti- β Tubulin (1:250; Cell Signaling #2128).

Statistical analysis

All results are expressed as mean \pm SEM. Results were analyzed by Student *t* test or ANOVA. Unpaired Student's *t* test and one-way analysis of variance were used for comparison of experimental groups. Statistical analysis is performed using GraphPad Prism software version 5.0b (GraphPad Software, Inc.). A probability value of less than 0.05 is considered significant.

Results

Cholesterol metabolism-related genes are differentially regulated in $\alpha\beta$ and $\gamma\delta$ T cells

Cholesterol is essential for maintaining proper permeability and fluidity in the cell membrane, and its level is tightly regulated within the cell. T cell proliferation is strongly linked to cellular cholesterol level and the regulation of genes involved in cholesterol metabolism [17]. To investigate whether cholesterol metabolism is differentially regulated in $\alpha\beta$ and $\gamma\delta$ T cell subsets, we examined the expression profiles of cholesterol-related pathway genes in $\alpha\beta$ and $\gamma\delta$ T cells from C57BL/6J mice with a pathway-based microarray. The result showed that many genes involved in esterification (*Acat1*, 2 and *Lcat*) or utilization (*Cyp39a1*, *Cyp46a1*, *Trefl*) of free cholesterol were upregulated in $\gamma\delta$ T cells. The expressions of *Pcsk9*, which downregulates LDLR posttranslationally [18], and *Abca1*, the main efflux transporter for cholesterol, were up-regulated in $\gamma\delta$ T cells as well (Fig. 1A). Genes relatively abundant and with significant fold-changes were confirmed in Taqman-based quantitative RT-PCR assays. Consistent with the

PCR array results, the $\gamma\delta$ T cells had a 1.6 fold increase in *Abca1*, a 3.4 fold increase in *Pcsk9*, a 2 fold increase in *Acat1*, a 4 fold increase in *Acat2*, a 2 fold increase in *Lcat*, and a 2.1 fold increase in *Trefl*, compared to $\alpha\beta$ T cells (Fig. 1B). These array data suggest that $\gamma\delta$ T cells express effort to lower free intracellular cholesterol levels by up-regulating genes involving in sterol efflux, esterification or other utilization pathways, possibly in response to higher intracellular cholesterol content.

Cholesterol content and lipid rafts are differentially regulated in $\alpha\beta$ and $\gamma\delta$ T cells

To investigate whether lipid and cholesterol levels are different in $\alpha\beta$ and $\gamma\delta$ T cells, we used Nile Red as a probe to detect neutral lipids (consisting mostly of cholesteryl ester and triglyceride [19,20]). $\gamma\delta$ T cells showed a significant increase in Nile Red staining compared to $\alpha\beta$ T cells, indicating that $\gamma\delta$ T cells contained more neutral lipid (Fig. 2A). We next specifically measured cholesterol levels in the two subsets. Resting $\alpha\beta$ and $\gamma\delta$ T cells were purified from C57BL/6J mice, and the intracellular cholesterol content in each subset was measured by gas chromatography. Interestingly, we found that the total intracellular cholesterol content was significantly higher in $\gamma\delta$ T cells (0.39 ± 0.03 vs 0.22 ± 0.00 μ g/ 10^6 cells in $\alpha\beta$ T cells, $P < 0.05$). Levels of free cholesterol seemed higher in the $\gamma\delta$ T cells, but the difference did not reach statistical significance. Cholesteryl ester levels were also higher in $\gamma\delta$ T cells (0.18 ± 0.05 vs 0.01 ± 0.04 μ g/ 10^6 cells in $\alpha\beta$ T cells, $P < 0.05$) (Fig. 2B). The increase in cholesteryl ester content correlates with the increase in intracellular neutral lipids observed by Nile Red staining of $\gamma\delta$ T cells. Average cell diameter appeared to be the same for $\alpha\beta$ and $\gamma\delta$ T cells (6.39 ± 0.05 vs 6.45 ± 0.02 μ m in $\alpha\beta$ T cells, $P = 0.222$), hence the increased intracellular cholesterol level was not due to a larger cell size of $\gamma\delta$ T cells (Fig. 2C).

Cholesterol is an indispensable component of membrane lipid rafts, which modulate TCR signaling by clustering proteins involved in TCR signaling. Perturbation of lipid rafts has been shown to interfere with T cell activation [21,22,23]. To learn whether the increase in cholesterol levels in $\gamma\delta$ T cells impacted their membrane lipid raft content, fluorescently-labeled CT-B, which binds to an essential raft-associated protein, GM1, was used to quantify lipid rafts on the plasma membrane [14,24]. Approximately 2-fold more CT-B bound to the plasma membrane of $\gamma\delta$ compared to $\alpha\beta$ cells, suggesting an increase in plasma membrane lipid raft content in $\gamma\delta$ cells (Fig. 2D). Microscopic images of CT-B staining also clearly showed more aggregation of lipid rafts on the plasma membranes of $\gamma\delta$ cells (Fig. 2E). Aggregation of lipid rafts and raft-associated proteins is positively associated with TCR signaling and T cell activation [23]. Taken together, these data suggest that higher cholesterol content in $\gamma\delta$ cells results in increased membrane lipid raft content, which could in turn, change TCR signaling in the $\gamma\delta$ T cells.

Cholesterol depletion reduces the activated phenotype of $\gamma\delta$ T cells

To confirm that the increased cholesterol content of $\gamma\delta$ cells results in enrichment of membrane lipid rafts, which in turn would likely impact TCR signaling and activation, we manipulated cholesterol levels in $\alpha\beta$ and $\gamma\delta$ T cells and examined their lipid raft content and activation status *in vitro*. Examination of surface markers shows $\gamma\delta$ T cells possess an activated status *in vivo* (increased percentages of CD44^{hi} CD62L⁻ and CD69⁺ cells) (Fig. 3A–B). The enhanced activation of $\gamma\delta$ T cells again suggests that these cells are more “primed for action” at baseline or resting.

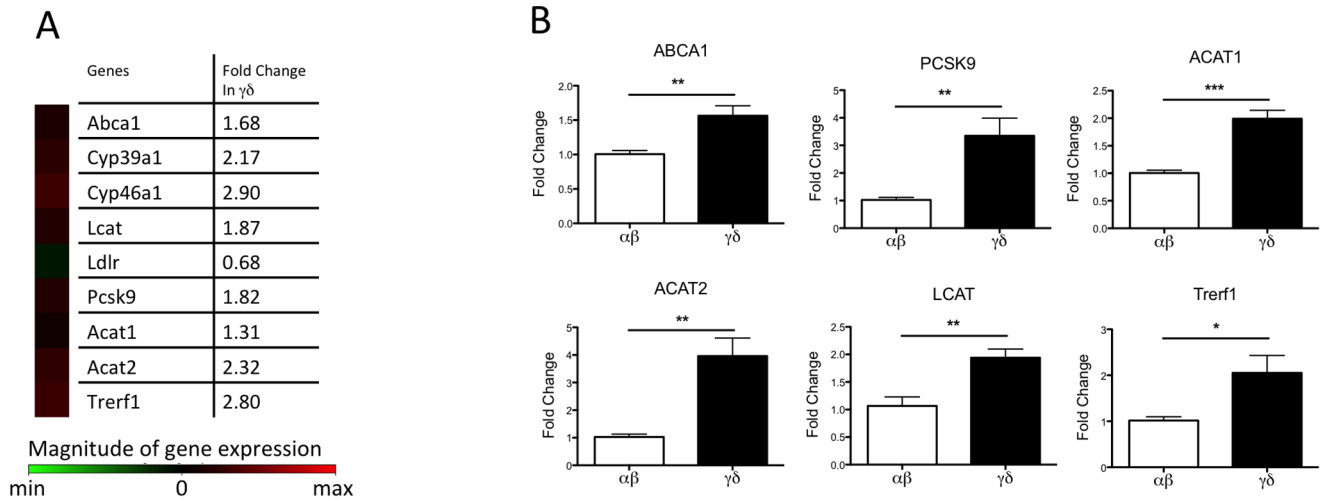


Figure 1. Cholesterol metabolism is differentially regulated in $\alpha\beta$ and $\gamma\delta$ T cells. (A) Heat map of sterol PCR array. Genes involved in sterol esterification, utilization, and efflux are upregulated in $\gamma\delta$ T cells. Gene expression of $\alpha\beta$ T cells was used as control to calculate fold change and hence not shown in the heat map. $\alpha\beta$ and $\gamma\delta$ T cells were isolated from spleens of the same female C57BL/6J mice by immuno-magnetic beads. (B) Quantitative RT-PCR analysis of genes regulating sterol metabolism. mRNA was isolated from $\alpha\beta$ and $\gamma\delta$ T cells from the same female C57BL/6J mice, and gene expression was detected by Taqman-based assays. *Gapdh* was used to normalize gene expression, and gene expression in $\alpha\beta$ T cells were set as 1. N=6. One sample was pooled from 3 mouse spleens. Results were shown in mean \pm SEM. * P<0.05, ** P<0.01, *** P<0.001. doi:10.1371/journal.pone.0063746.g001

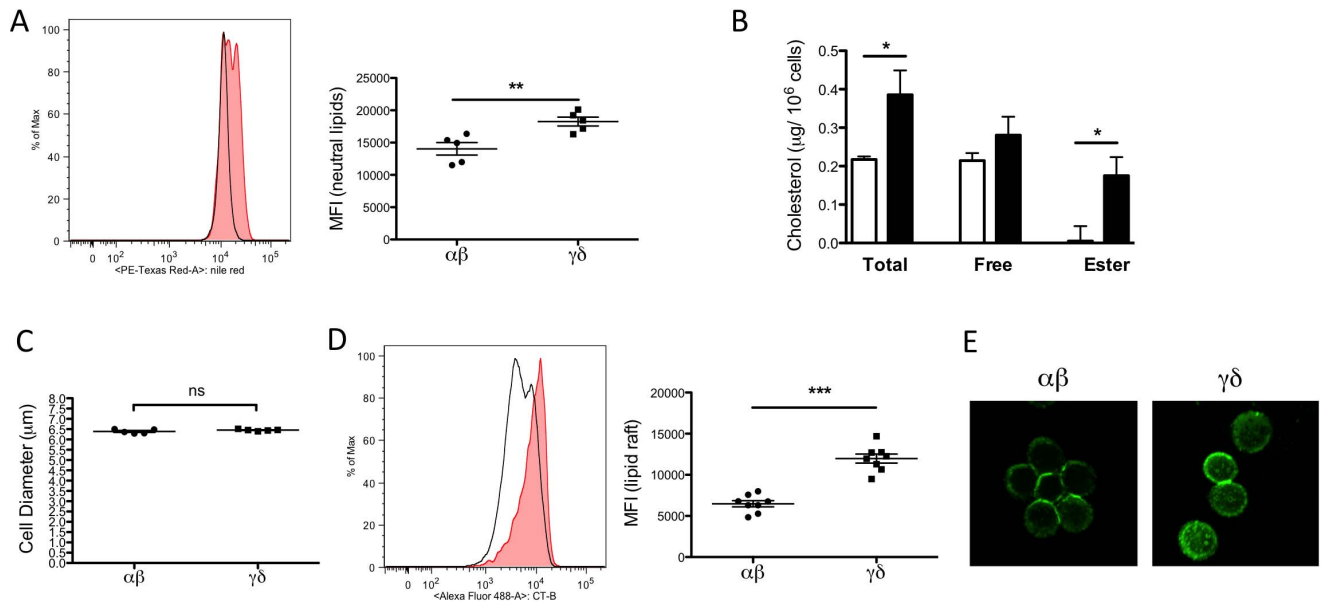


Figure 2. $\gamma\delta$ T cells have increased intracellular neutral lipids, cholesterol, and lipid rafts. (A) Splenocytes were isolated from C57BL/6J mice. Intracellular lipid was quantified by Nile Red staining. Left: A representative plot shows the relative intensity of Nile Red staining on $\alpha\beta$ (solid black line) and $\gamma\delta$ (tinted shade) T cells. Right: Graph shows the median fluorescent intensity of Nile Red staining on $\alpha\beta$ and $\gamma\delta$ T cells. Results were averaged from 5 mice, and shown in mean \pm SEM. (B) Total and free cholesterol was quantified in purified $\alpha\beta$ (white) and $\gamma\delta$ (black) T cells from C57BL/6J mouse spleens by gas chromatography. Cholesteryl ester was calculated as the difference between total and free cholesterol (multiplied by 1.67). Intracellular total cholesterol and cholesteryl ester content is significantly higher in $\gamma\delta$ T cells. Cholesterol level was normalized to cell numbers. N=5. (C) $\alpha\beta$ and $\gamma\delta$ T cells were isolated from splenocytes of C57BL/6J mice. Average cell diameters were obtained from a Multisizer IV Coulter Counter (Beckman Coulter) and showed no significant difference (ns) in $\alpha\beta$ and $\gamma\delta$ T cells. Results were averaged from 5 mice, and shown in mean \pm SEM. (D) Staining for GM1 shows significantly higher lipid raft content on the plasma membrane of $\gamma\delta$ T cells. Splenocytes were isolated from C57BL/6J mice. GM1 of lipid raft was identified by cholera toxin subunit B (CT-B) binding. Left: A representative plot shows the relative intensity of CT-B staining on $\alpha\beta$ (solid black line) and $\gamma\delta$ (tinted shade) T cells. Right: Graph shows the median fluorescent intensity of CT-B staining on $\alpha\beta$ and $\gamma\delta$ T cells. Results were averaged from 8 mice. Results were shown in mean \pm SEM. * P<0.05, ** P<0.01, *** P<0.001. (E) Confocal microscopic images show increased lipid rafts staining on the membrane of $\gamma\delta$ T cells (300 \times). Green: GM1. doi:10.1371/journal.pone.0063746.g002

$\alpha\beta$ and $\gamma\delta$ T cells from C57BL/6J spleen were stimulated with α CD3/CD28 antibodies in the absence or presence of methyl β -cyclodextrin (M β CD) to remove cellular cholesterol [25]. Lipid raft content and T cells activation markers were assessed by flow cytometry. Compared to $\alpha\beta$ T cells, $\gamma\delta$ T cells have a higher lipid raft content in the absence of M β CD ($P < 0.05$). In cells treated with M β CD, the lipid raft content was lowered to similar levels in both $\alpha\beta$ and $\gamma\delta$ T cells (Fig. 3C). After incubation with M β CD for 4 hours, we observed a reduction in percentages of CD44^{hi}CD62L⁻ $\gamma\delta$ cells, but not $\alpha\beta$ cells (Fig. 3D). With 4 hours of M β CD treatment, we found a slight but not significant reduction of early T cell activation marker CD69 (Fig. 3E). However, at 2 hours of cholesterol depletion, CD69⁺ cells were significantly lowered in only the $\gamma\delta$ cells ($P < 0.01$) (Fig. 3E, inset). We reasoned that since CD69 is one of the earliest expressed markers in T cell activation [26], its expression pattern may reflect T cell activation status early upon stimulation. We also used cholesterol-loaded cyclodextrin to enhance cellular cholesterol content in $\alpha\beta$ and $\gamma\delta$ T cells [27,28]. Interestingly, we found that the percentage of CD44^{hi}CD62L⁻ cells was significantly increased in $\alpha\beta$ T cells in a dose-dependent manner with cholesterol addition. On the other hand, activated $\gamma\delta$ T cells were gradually reduced with excess cholesterol, possibly due to oversaturation of membrane cholesterol (Fig. 3F). The fact that $\alpha\beta$ T cells, which had less cellular cholesterol at baseline, became activated with cholesterol loading supports the idea that increased cholesterol content leads to the primed phenotype in T cells.

$\gamma\delta$ T cells are more proliferative and show enhanced basal ERK1/2 phosphorylation

$\gamma\delta$ T cells play a critical role in the initial stages of various pathophysiological conditions. Compared to conventional $\alpha\beta$ T cells, $\gamma\delta$ T cells respond much faster when faced with microbial and tumor invasions [4,29]. Indeed, we found a significant increase in BrdU incorporation in $\gamma\delta$ T cells ($2.67 \pm 0.09\%$ of total $\gamma\delta^+$) from C57BL/6J mouse spleen compared to $\alpha\beta$ T cells ($0.79 \pm 0.02\%$ of total $\alpha\beta^+$, $P < 0.001$) (Fig. 4A). Together with the increased expression of activation markers (Fig. 3A–B), our data suggesting that $\gamma\delta$ T cells possess a more “primed for action” status at baseline in the absence of any external stimulation.

Next, we wanted to investigate the molecular mechanisms by which cholesterol stimulates $\gamma\delta$ T cell activation. Because the accumulated cholesterol favors lipid raft formation, which could modulate TCR signaling, we first considered the possibility that $\gamma\delta$ T cells had a lower TCR threshold [23]. To examine this hypothesis, we stimulated resting $\alpha\beta$ and $\gamma\delta$ T cells with a fixed concentration of soluble α CD28 and an increasing concentration of plate-bound α CD3 antibodies, and measured proliferation using CFSE dilution [14]. We found that $\gamma\delta$ T cells are more proliferative at the higher α CD3 concentration (Fig. 4B, top). However, when the log scaling of α CD3 concentration versus percentage of maximum response was plotted to determine the EC₅₀ values, we did not see a significant difference in TCR threshold between $\alpha\beta$ and $\gamma\delta$ T cells (Fig. 4B, lower). Our data suggest that an enhanced TCR signaling strength, but not a lower TCR threshold, likely accounts for the cholesterol-induced activation and proliferation in $\gamma\delta$ T cells. We also noticed that with no or lower levels of α CD3 stimulation, membrane CD3 expression was significantly higher in $\gamma\delta$ T cells compared to $\alpha\beta$ T cells. This again indicates a stronger TCR signaling in the $\gamma\delta$ T cells basally or with low levels of stimulation. However, the expression of CD3 was downregulated and gradually became indifferent in both $\alpha\beta$ and $\gamma\delta$ T cells under stronger stimulation (Fig. 4C)

To determine whether basal TCR signaling is indeed increased in the $\gamma\delta$ T cells, we stimulated purified resting $\alpha\beta$ and $\gamma\delta$ T cells with α CD3 and α CD28 antibodies, and examined the phosphorylation status of ERK1/2, a well-studied TCR downstream effector for proliferation [30,31]. We found an increase in basal ERK1/2 phosphorylation in unstimulated $\gamma\delta$ T cells, compared to almost no basal phosphorylation in $\alpha\beta$ T cells (Fig. 4D). The enhanced ERK1/2 phosphorylation likely accounts for the increased proliferation and activation of $\gamma\delta$ T cells in the resting status (Fig. 3A–B, 4A).

Enhanced TCR signaling and ERK1/2 phosphorylation lead to T cell hyperplasia. To confirm that enhanced ERK1/2 signaling accounts, at least in part, for the hyperproliferative phenotype of $\gamma\delta$ T cells, we performed an *in vitro* proliferation assay in the presence of an ERK1/2 inhibitor, U0126. Indeed, U0126 incubation significantly inhibited $\gamma\delta$ T cell proliferation in a dose-dependent manner. However, under the same condition, the overall growth inhibition effect was not significant in the $\alpha\beta$ T cells (Fig. 4E). The results provide further evidence that enhanced ERK1/2 signaling contributes to the hyperproliferative phenotype of $\gamma\delta$ T cells.

Discussion

$\alpha\beta$ and $\gamma\delta$ T cells share many common features, yet are functionally and metabolically distinct. For example, expression of activation markers, cytokines, and TCR signaling pathways are very similar in the two subsets [32,33,34]. However, $\gamma\delta$ T cells are negative for both CD4 and CD8, and are MHC-independent in antigen recognition. Their rapid responses upon antigen encounter also distinguish them from $\alpha\beta$ T cells. $\gamma\delta$ cells are thought to be involved in innate immunity whereas $\alpha\beta$ cells are involved in adaptive immunity [2,3,4]. To date, very little is known about how antigen-naïve $\gamma\delta$ T cells hold the “primed for action” status and are able to become activated and proliferative in such a short period of time. In this report, we provide novel insights for the distinct phenotypes and differential regulation of $\alpha\beta$ and $\gamma\delta$ T cells. We showed that, in accordance with previous reports [35,36], $\gamma\delta$ T cells proliferate faster and are more activated than $\alpha\beta$ T cells at resting conditions (Fig. 3A–B and 4A). We found that $\gamma\delta$ T cells have significantly higher intracellular neutral lipid and cholesterol content (Fig. 2A–B). Furthermore, we found that the increased cholesterol content in $\gamma\delta$ T cells results in an increase in lipid raft formation (Fig. 2D–E), which favors TCR clustering and signaling. The enhanced TCR signaling is demonstrated by elevated ERK1/2 phosphorylation, proliferation, and activation marker expression in $\gamma\delta$ T cells (Fig. 3A–B, 4A, D). Thus, $\gamma\delta$ T cells are kept in a “primed for action” status at a resting state, and are ready to undergo rapid proliferation and activation. We show that cholesterol, at least in part, modulates their function.

One of the best-studied functions of lipid rafts is the regulation of TCR signaling. By clustering TCR molecules and their associated factors, lipid rafts provide a concentrated and stable signaling micro-domain for TCR-dependent T cell activation [22,23,37]. Cholesterol, a key component of lipid rafts, is indispensable for TCR-dependent functions, and the modulation of cholesterol levels tightly correlates with the strength of TCR signaling. For example, cholesterol depletion of lymphocytes results in reduced raft domains and subsequent dysregulated T cell signaling [38]. On the other hand, a recent study showed that enriching membrane cholesterol by squalene enhances the responses of CD4⁺ T cells *in vivo* [13]. The hyper-activation of T cells in the autoimmune disease systemic lupus erythematosus is likely caused by high cholesterol-induced lowering of the TCR

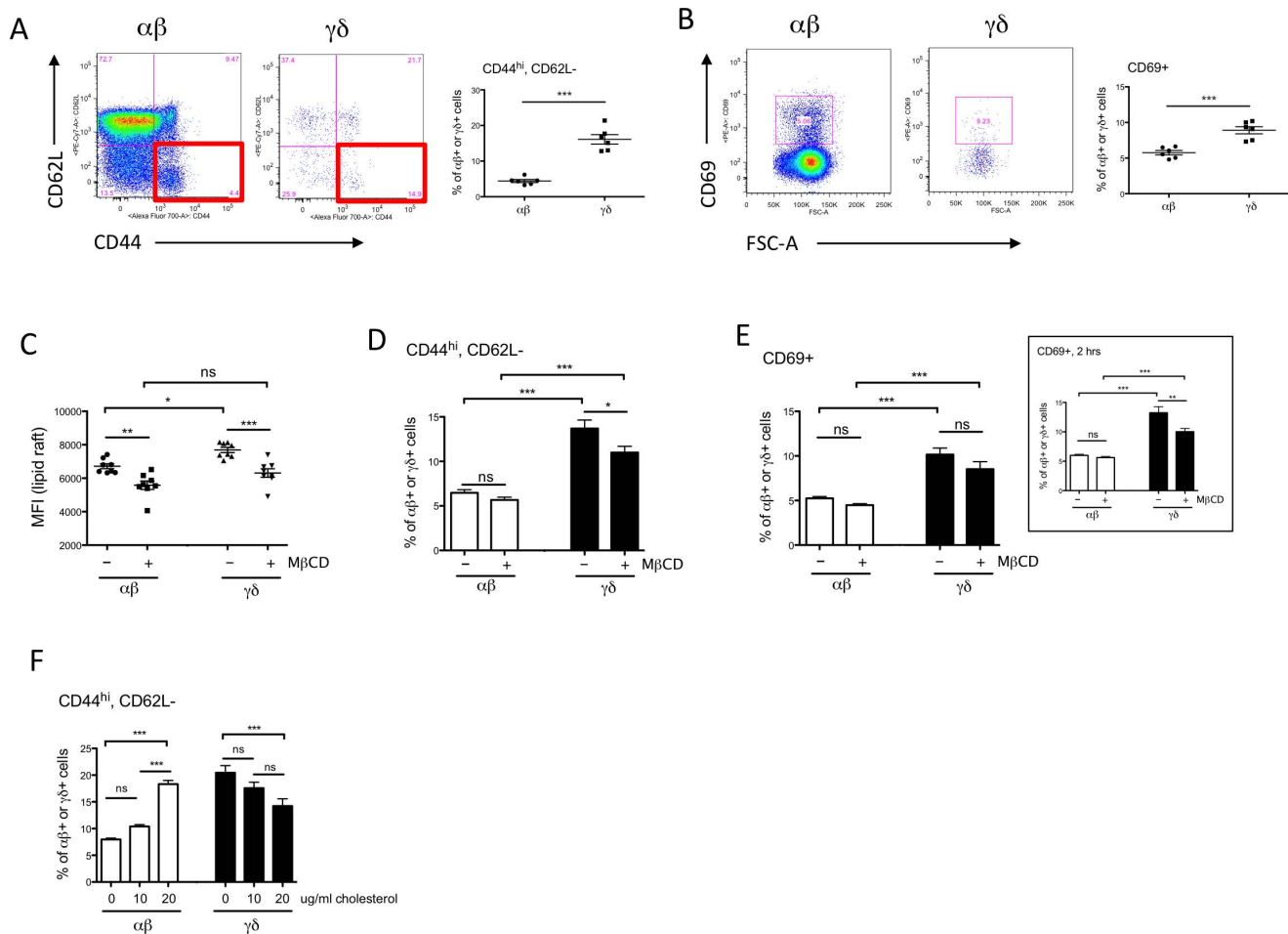


Figure 3. $\gamma\delta$ T cells are more activated *in vivo*. Cholesterol depletion reduces the activated phenotype of $\gamma\delta$ T cells. Cholesterol addition significantly increases the activation status of $\alpha\beta$ T cells. (A–B) Staining of T cell activation markers shows more $\gamma\delta$ T cell are in the activated state *in vivo*, comparing to $\alpha\beta$ T cells. Splenocytes were isolated from C57BL/6J mice. T cell activation was identified by (A) CD44^{hi} CD62L⁻ and (B) CD69⁺ cells. Representative flow cytometric plots are shown on the left and the percentages of activated T cells are graphed on the right. Results were averaged from 6 mice, and shown in mean \pm SEM. (C–E) Splenocytes from C57BL/6J were stimulated with T-activator CD3/CD28 beads for 4 hours in the presence or absence of M β CD to remove cholesterol from the plasma membrane. (C) Reduction of lipid raft levels in $\alpha\beta$ and $\gamma\delta$ T cells with cholesterol depletion. The reduction was more significant in $\gamma\delta$ T cells, and the difference in lipid raft level became insignificant in $\alpha\beta$ and $\gamma\delta$ T cells after M β CD treatment. Lipid raft content was expressed in median florescent intensity of CT-B staining. (D) The percentage of CD44^{hi} CD62L⁻ cells was significantly lower in $\gamma\delta$ T cells after 4 hours of cholesterol depletion. (E) The difference in expression of early activation marker CD69 was not statistically significant in both $\alpha\beta$ or $\gamma\delta$ T cells after M β CD treatment for 4 hours. However, the reduction of CD69 was significant in $\gamma\delta$ T cells at 2 hours (inset). Results were shown in mean \pm SEM. (F) C57BL/6J splenocytes were stimulated with T-activator CD3/CD28 beads in the presence or absence of 10 and 20 μ g/ml cholesterol for 4 hours. The percentage of CD44^{hi}CD62L⁻ cells was significantly increased in $\alpha\beta$ T cells in a dose-dependent manner of cholesterol addition. On the other hand, activated $\gamma\delta$ T cells were reduced with excess cholesterol. Results were averaged from 8 mice and shown in mean \pm SEM. * $P < 0.05$; ** $P < 0.01$; *** $P < 0.001$; ns not statistically significant. doi:10.1371/journal.pone.0063746.g003

threshold [21]. Due to the increase in cholesterol content in $\gamma\delta$ cells, we initially hypothesized that their hyper-active phenotype was caused by a lowered TCR threshold [23]. However, to our surprise, we found that the TCR thresholds were similar in $\alpha\beta$ and $\gamma\delta$ T cells *in vitro* (Fig. 4B). The higher membrane CD3 expression of $\gamma\delta$ T cells under no or low stimulation suggested an enhanced basal TCR strength in these cells (Fig. 4C). The enhanced TCR signaling is confirmed by increased level of ERK1/2 phosphorylation in $\gamma\delta$ T cells at the resting state (Fig. 4D). Thus, our data supports the model that the increased intracellular cholesterol content favors lipid raft formation and enhanced TCR signaling strength in $\gamma\delta$ T cells. Our data also provide direct evidence linking high intracellular cholesterol level to the activation of $\gamma\delta$ T cells. M β CD-mediated cholesterol depletion lowers the lipid raft

content of $\gamma\delta$ to the same level as $\alpha\beta$ T cells, and significantly attenuated the expression of activation markers in $\gamma\delta$ T cells (Fig. 3C–E). On the other hand, increasing cellular cholesterol enhanced the activation status of $\alpha\beta$ T cells (Fig. 3F). The cholesterol depletion and loading studies support the notion that cellular cholesterol content directly and positively impacts T cell activation.

Our data provides novel evidence that elevated cellular cholesterol content contributes to rapid proliferation and activation of $\gamma\delta$ T cells, which are well-recognized hallmarks of these cells [35]. However, the mechanism by which cholesterol accumulates in $\gamma\delta$ T cells requires further investigation. More studies are underway to explore what factors/signaling pathways are involved in this process. $\gamma\delta$ T cells are potent producers of

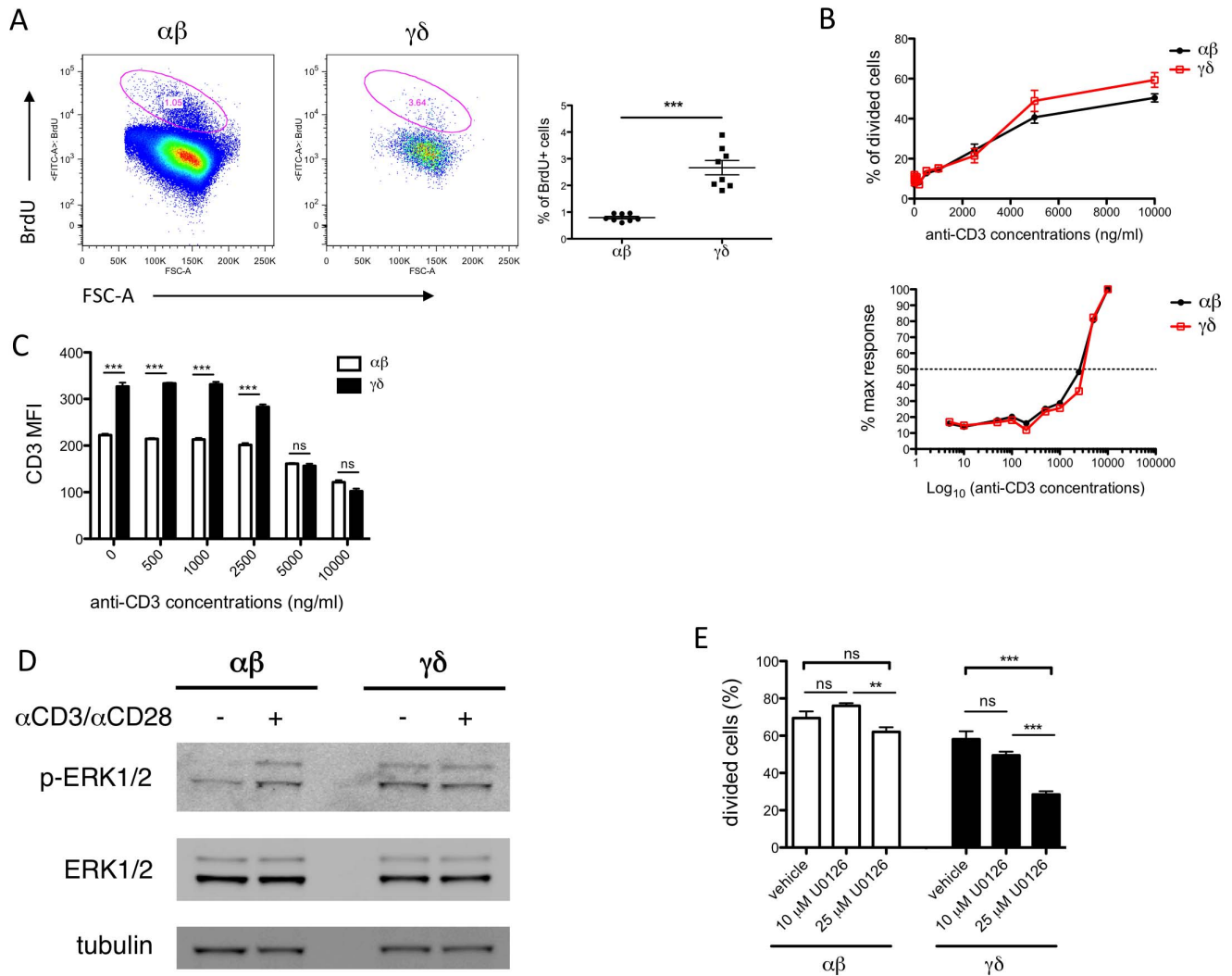


Figure 4. $\gamma\delta$ T cells have similar TCR threshold but enhanced ERK1/2 phosphorylation comparing to $\alpha\beta$ T cells. (A) Percentages of BrdU⁺ proliferative cells are higher in the $\gamma\delta$ T cell subset *in vivo*. Left: representative plots of BrdU⁺ populations (circled) in $\alpha\beta$ and $\gamma\delta$ T cells. Right: Graph of percentages of BrdU⁺ cells in $\alpha\beta$ and $\gamma\delta$ T cells. C57BL/6J mice received single dose of BrdU (1 mg) via intraperitoneal injection, and splenocytes were isolated 3 days later. BrdU⁺ cells were identified by fluorescently labeled anti-BrdU antibody and flow cytometry. Results were averaged from 8 mice, and shown in mean \pm SEM. *** $P < 0.001$. (B) Top: Splenocytes from C57BL/6J mice were labeled with CFSE (2.5 μ M), and then stimulated with 0–10 μ g/ml plate-bound α CD3 and 1 μ g/ml soluble α CD28 for 24 hours. CFSE content in cells was measured by flow cytometry and graphed against α CD3 concentrations. Results were averaged from 5 mice, and shown in mean \pm SEM. Lower: Log scaling of α CD3 concentration against % of maximum response was used to calculate EC₅₀. (C) CD3 expression in $\gamma\delta$ T cells was higher than in $\alpha\beta$ T cells under no or lower stimulation, but decreased more dramatically with stronger stimulation. The experimental condition was the same as in (B). (D) Western blotting shows high levels of phosphorylated ERK1/2 in $\gamma\delta$ T cells, relative to $\alpha\beta$ T cells, at baseline. $\alpha\beta$ and $\gamma\delta$ T cells were isolated from the same set of C57BL/6J mice via FACS sorting. Cells were either untreated, or incubated with α CD3 and α CD28 antibodies (20 μ g/ml each) for 5 minutes and then with anti-hamster IgG (20 μ g/ml) for additional 2 minutes at 37°C. Cells were lysed, separated by SDS-PAGE, and immunoblotted with indicated antibodies. The image was representative of 3 independent experiments. (E) Inhibition of ERK1/2 significantly lowers proliferation in $\gamma\delta$ T cells *in vitro*. Splenocytes from C57BL/6J mice were labeled with CFSE (2.5 μ M), and then stimulated with 1 μ g/ml plate-bound α CD3 and 1 μ g/ml soluble α CD28 for 24 hours, in the absence (vehicle) or presence of 10 μ M and 25 μ M U0126. CFSE dilution in cells was measured by flow cytometry, and used to calculate cell proliferation. Results were averaged from 7–8 mice, and shown in mean \pm SEM. ** $P < 0.01$; *** $P < 0.001$; ns not statistically significant. doi:10.1371/journal.pone.0063746.g004

effector cytokines such as IL-17 and IFN γ [39]. The fate of IL-17- or IFN γ -producing subsets is pre-determined by CD27 and other factors such as TGF β in the thymus [36,40,41]. The two subsets are differentially regulated and respond to different stimuli [42,43]. For example, antigen-naïve $\gamma\delta$ T cells predominantly produce IL-17 for neutrophil recruitment and resolution of early infection. On the other hand, antigen-experienced $\gamma\delta$ T cells produce IFN γ at the site of infection [44]. Particularly, $\gamma\delta$ T cells are found to be the major source of IL-17 in naïve mice, and IL-17

production by $\gamma\delta$ cells can be further modulated in various pathological conditions including atherosclerosis [36,40,43,45,46]. Although $\gamma\delta$ cells have not been directly studied in atherosclerosis, given that atherosclerosis is driven by both cholesterol and T cells, it would be interesting to study whether cholesterol regulates $\gamma\delta$ subset determination, and whether $\gamma\delta$ T cells play a pivotal role in atherogenesis. For instance, increased cholesterol levels may favor the development of a specific $\gamma\delta$ subset or further regulate its responsiveness to stimuli. We plan to investigate whether the

development of $\gamma\delta$ T cell subsets, as well as the effectiveness and activation of these subsets are affected by elevating cholesterol levels *in vivo*.

In sum, $\gamma\delta$ T cells are more proliferative and activated than $\alpha\beta$ cells *in vivo*, suggesting $\gamma\delta$ cells are at a more “primed for action” status. The increased cholesterol content of $\gamma\delta$ T cells suggests that $\gamma\delta$ are able to reach the cholesterol checkpoint faster to allow for rapid proliferation and activation [17]. In addition, increased cholesterol levels in the cell resulted in a higher lipid raft content, which promoted $\gamma\delta$ T cell activation. Cholesterol depletion experiments confirmed that both lipid raft content and activation markers were perturbed in cholesterol-depleted $\gamma\delta$ T cells, thus further proving that intracellular cholesterol levels are key to $\gamma\delta$ activation. $\gamma\delta$ T cells were shown to have the same TCR threshold as $\alpha\beta$ T cells. However, ERK1/2, the key downstream effector of TCR signaling, is heavily phosphorylated in unstimulated $\gamma\delta$ T cells, and ERK1/2 inhibition effectively reduced $\gamma\delta$ T cell

proliferation, suggesting that the “primed for action” phenotype of $\gamma\delta$ T cells is the result of enhanced TCR signaling strength due to increased cholesterol content. Taken together, our data provide a novel mechanism by which cholesterol differentially regulates the physiology of $\alpha\beta$ and $\gamma\delta$ T cell subsets.

Acknowledgments

We thank Amy Blatchley for technical assistance, and the flow cytometry facility at the La Jolla Institute for Allergy and Immunology for data analysis support and cell sorting.

Author Contributions

Conceived and designed the experiments: HYC CCH. Performed the experiments: HYC RW AKG RNH DJS. Analyzed the data: HYC JSP CCH. Contributed reagents/materials/analysis tools: JSP KL. Wrote the paper: HYC CCH.

References

- Inghirami G, Zhu BY, Chess L, Knowles DM (1990) Flow cytometric and immunohistochemical characterization of the gamma/delta T-lymphocyte population in normal human lymphoid tissue and peripheral blood. *The American journal of pathology* 136: 357–367.
- Champagne E (2011) gammadelta T cell receptor ligands and modes of antigen recognition. *Archivum immunologiae et therapeuticae experimentalis* 59: 117–137.
- Kapsenberg ML (2009) Gammadelta T cell receptors without a job. *Immunity* 31: 181–183.
- Eberl M, Moser B (2009) Monocytes and gammadelta T cells: close encounters in microbial infection. *Trends in immunology* 30: 562–568.
- Fang H, Welte T, Zheng X, Chang GJ, Holbrook MR, et al. (2010) gammadelta T cells promote the maturation of dendritic cells during West Nile virus infection. *FEMS immunology and medical microbiology* 59: 71–80.
- Brandes M, Willmann K, Biele G, Levy N, Eberl M, et al. (2009) Cross-presenting human gammadelta T cells induce robust CD8+ alphabeta T cell responses. *Proceedings of the National Academy of Sciences of the United States of America* 106: 2307–2312.
- Graff JC, Behnke M, Radke J, White M, Jutila MA (2006) A comprehensive SAGE database for the analysis of gammadelta T cells. *Int Immunol* 18: 613–626.
- Shires J, Theodoridis E, Hayday AC (2001) Biological insights into TCRgammadelta+ and TCRalphabeta+ intraepithelial lymphocytes provided by serial analysis of gene expression (SAGE). *Immunity* 15: 419–434.
- Laird RM, Hayes SM (2009) Profiling of the early transcriptional response of murine gammadelta T cells following TCR stimulation. *Mol Immunol* 46: 2429–2438.
- Fahrer AM, Konigshofer Y, Kerr EM, Ghandour G, Mack DH, et al. (2001) Attributes of gammadelta intraepithelial lymphocytes as suggested by their transcriptional profile. *Proc Natl Acad Sci U S A* 98: 10261–10266.
- Jameson JM, Cruz J, Costanzo A, Terajima M, Ennis FA (2010) A role for the mevalonate pathway in the induction of subtype cross-reactive immunity to influenza A virus by human gammadelta T lymphocytes. *Cellular immunology* 264: 71–77.
- Gombos I, Kiss E, Detre C, Laszlo G, Matko J (2006) Cholesterol and sphingolipids as lipid organizers of the immune cells' plasma membrane: their impact on the functions of MHC molecules, effector T-lymphocytes and T-cell death. *Immunol Lett* 104: 59–69.
- Surls J, Nazarov-Stoica C, Kehl M, Olsen C, Casares S, et al. (2012) Increased Membrane Cholesterol in Lymphocytes Diverts T-Cells toward an Inflammatory Response. *PLoS one* 7: e38733.
- Armstrong AJ, Gebre AK, Parks JS, Hedrick CC (2010) ATP-binding cassette transporter G1 negatively regulates thymocyte and peripheral lymphocyte proliferation. *J Immunol* 184: 173–183.
- Major AS, Wilson MT, McCaleb JL, Ru Su Y, Stanic AK, et al. (2004) Quantitative and qualitative differences in proatherogenic NKT cells in apolipoprotein E-deficient mice. *Arteriosclerosis, thrombosis, and vascular biology* 24: 2351–2357.
- Rudel LL, Kelley K, Sawyer JK, Shah R, Wilson MD (1998) Dietary monounsaturated fatty acids promote aortic atherosclerosis in LDL receptor-null, human ApoB100-overexpressing transgenic mice. *Arteriosclerosis, thrombosis, and vascular biology* 18: 1818–1827.
- Bensinger SJ, Bradley MN, Joseph SB, Zelcer N, Janssen EM, et al. (2008) LXR signaling couples sterol metabolism to proliferation in the acquired immune response. *Cell* 134: 97–111.
- Zhang DW, Garuti R, Tang WJ, Cohen JC, Hobbs HH (2008) Structural requirements for PCSK9-mediated degradation of the low-density lipoprotein receptor. *Proceedings of the National Academy of Sciences of the United States of America* 105: 13045–13050.
- Greenspan P, Mayer EP, Fowler SD (1985) Nile red: a selective fluorescent stain for intracellular lipid droplets. *The Journal of cell biology* 100: 965–973.
- Diaz G, Melis M, Batetta B, Angius F, Falchi AM (2008) Hydrophobic characterization of intracellular lipids in situ by Nile Red red/yellow emission ratio. *Micron* 39: 819–824.
- Jury EC, Kabouridis PS, Flores-Borja F, Mageed RA, Isenberg DA (2004) Altered lipid raft-associated signaling and ganglioside expression in T lymphocytes from patients with systemic lupus erythematosus. *J Clin Invest* 113: 1176–1187.
- Jury EC, Flores-Borja F, Kabouridis PS (2007) Lipid rafts in T cell signalling and disease. *Semin Cell Dev Biol* 18: 608–615.
- Kabouridis PS, Jury EC (2008) Lipid rafts and T-lymphocyte function: implications for autoimmunity. *FEBS Lett* 582: 3711–3718.
- Lu HZ, Zhu AY, Chen Y, Tang J, Li BQ (2011) Formation and aggregation of lipid rafts in gammadelta T cells following stimulation with Mycobacterium tuberculosis antigens. *The Tohoku journal of experimental medicine* 223: 193–198.
- Fulop T, Jr., Douziech N, Goulet AC, Desgeorges S, Linteau A, et al. (2001) Cycloclextrin modulation of T lymphocyte signal transduction with aging. *Mech Ageing Dev* 122: 1413–1430.
- Wang X, Xu H, Alvarez X, Pahar B, Moroney-Rasmussen T, et al. (2011) Distinct expression patterns of CD69 in mucosal and systemic lymphoid tissues in primary SIV infection of rhesus macaques. *PLoS one* 6: e27207.
- Whetzel AM, Sturek JM, Nagelin MH, Bolick DT, Gebre AK, et al. (2010) ABCG1 deficiency in mice promotes endothelial activation and monocyte-endothelial interactions. *Arterioscler Thromb Vasc Biol* 30: 809–817.
- Tarling EJ, Edwards PA (2011) ATP binding cassette transporter G1 (ABCG1) is an intracellular sterol transporter. *Proceedings of the National Academy of Sciences of the United States of America* 108: 19719–19724.
- Moser B, Eberl M (2011) gammadelta T-APCs: a novel tool for immunotherapy? *Cellular and molecular life sciences : CMLS* 68: 2443–2452.
- Chen Y, Ci X, Gorentla B, Sullivan SA, Stone JC, et al. (2012) Differential Requirement of RasGRP1 for gammadelta T Cell Development and Activation. *Journal of immunology* 189: 61–71.
- Li D, Moldrem JJ, Ma Q (2009) LFA-1 regulates CD8+ T cell activation via T cell receptor-mediated and LFA-1-mediated Erk1/2 signal pathways. *The Journal of biological chemistry* 284: 21001–21010.
- Wong GW, Zuniga-Pflucker JC (2010) gammadelta and alphabeta T cell lineage choice: resolution by a stronger sense of being. *Seminars in immunology* 22: 228–236.
- Born WK, Yin Z, Hahn YS, Sun D, O'Brien RL (2010) Analysis of gamma delta T cell functions in the mouse. *Journal of immunology* 184: 4055–4061.
- Gao YL, Rajan AJ, Raine CS, Brosnan CF (2001) gammadelta T cells express activation markers in the central nervous system of mice with chronic-relapsing experimental autoimmune encephalomyelitis. *J Autoimmun* 17: 261–271.
- Tough DF, Sprent J (1998) Lifespan of gamma/delta T cells. *The Journal of experimental medicine* 187: 357–365.
- Do JS, Fink PJ, Li L, Spolski R, Robinson J, et al. (2010) Cutting edge: spontaneous development of IL-17-producing gamma delta T cells in the thymus occurs via a TGF-beta 1-dependent mechanism. *Journal of immunology* 184: 1675–1679.
- Kenworthy AK (2008) Have we become overly reliant on lipid rafts? Talking Point on the involvement of lipid rafts in T-cell activation. *EMBO reports* 9: 531–535.
- Kabouridis PS, Janzen J, Magee AL, Ley SC (2000) Cholesterol depletion disrupts lipid rafts and modulates the activity of multiple signaling pathways in T lymphocytes. *European journal of immunology* 30: 954–963.

39. Jensen KD, Chien YH (2009) Thymic maturation determines gammadelta T cell function, but not their antigen specificities. *Curr Opin Immunol* 21: 140–145.
40. Jensen KD, Su X, Shin S, Li L, Youssef S, et al. (2008) Thymic selection determines gammadelta T cell effector fate: antigen-naive cells make interleukin-17 and antigen-experienced cells make interferon gamma. *Immunity* 29: 90–100.
41. Ribot JC, deBarros A, Pang DJ, Neves JF, Peperzak V, et al. (2009) CD27 is a thymic determinant of the balance between interferon-gamma- and interleukin 17-producing gammadelta T cell subsets. *Nature immunology* 10: 427–436.
42. Ribot JC, Chaves-Ferreira M, d'Orey F, Wencker M, Goncalves-Sousa N, et al. (2010) Cutting edge: adaptive versus innate receptor signals selectively control the pool sizes of murine IFN-gamma- or IL-17-producing gammadelta T cells upon infection. *Journal of immunology* 185: 6421–6425.
43. Martin B, Hirota K, Cua DJ, Stockinger B, Veldhoen M (2009) Interleukin-17-producing gammadelta T cells selectively expand in response to pathogen products and environmental signals. *Immunity* 31: 321–330.
44. Sutton CE, Mielke LA, Mills KH (2012) IL-17-producing gammadelta T cells and innate lymphoid cells. *European journal of immunology* 42: 2221–2231.
45. Murdoch JR, Lloyd CM (2010) Resolution of allergic airway inflammation and airway hyperreactivity is mediated by IL-17-producing {gamma}{delta}T cells. *American journal of respiratory and critical care medicine* 182: 464–476.
46. Smith E, Prasad KM, Butcher M, Dobrian A, Kolls JK, et al. (2010) Blockade of interleukin-17A results in reduced atherosclerosis in apolipoprotein E-deficient mice. *Circulation* 121: 1746–1755.